Experimental Analysis of a Wideband Pattern Diversity Antenna with Compact Reconfigurable CPW-to-Slotline Transition Feed

Yue Li, Zhijun Zhang, *Senior Member, IEEE*, Jianfeng Zheng, Zhenghe Feng, Senior *Member, IEEE* and Magdy F. Iskander, *Fellow, IEEE*

***Abstract*—A wideband antenna with a reconfigurable coplanar waveguide (CPW)-to-slotline transition feed is proposed for pattern diversity applications. The feed provides three modes –CPW feed, left slotline (LS) feed and right slotline (RS) feed– without extra matching structures. Changes between modes are controlled by only two p-i-n diodes. Features of the proposed switchable feed include compact size and simple bias circuit. The equivalent transmission line model is used in the analysis of the proposed design. A prototype of the proposed antenna is fabricated, tested, and the obtained results including reflection coefficient, radiation patterns and gains, are present. A measurement of channel capacity is carried out to prove the benefit of pattern diversity when using the proposed antenna in both line-of-sight (LOS) and non-line-of-sight (NLOS) communication scenarios.**

***Index Terms*—Reconfigurable antennas, antenna feed, pattern diversity, wideband antennas, channel capacity.**

I. Introduction

With the rapid progress in developing advanced wireless communication systems, the advantages of using reconfigurable antenna patterns have been recognized and widely adopted in many designs. Reconfigurable antenna patterns provide pattern diversity that could be used to provide dynamic radiation coverage and mitigate multi-path fading. The diversity and increased directional gains of pattern reconfigurable antennas also improves coverage and increase the channel capacity, especially in the multiple antennas system [1-3]. Among the recent designs of such antenna systems is the research work published in [4-13]. One method to achieve reconfigurable pattern is to adjust the structure of the radiating element, including the antenna shape [4-5], shorting sections [6] and parasitic elements [7-8], dynamically. Another reconfigurable pattern solution may be achieved through the selection of the radiating elements [9-13]. In this case, radiating elements in different directions are electronically selected by switchable mechanism to achieve the desired directive beams [9-11].

In [12-13], a reconfigurable CPW-to-slotline transition is proposed and a compact antenna feed, supporting both the CPW and slotline feed is described. Such a transition presents an effective solution to the feeding of different radiating elements in a relatively compact dimension. Such a feed approach has been widely studied and applied in different configurations [12-16]. For example, in the design described in [14], the CPW feed was converted to slotline feed by adding a 180° phase shifter. Another method to design CPW-to-slotline transition is to short circuit one of the two slots of the CPW, and add a λ/4 transformer structure to avoid reflections from the shorted end and provide good impedance matching [12-13, 15]. In [13], the matching slot was used as a radiating element, while a function similar to a transformer was realized in [16] by using a CPW series stub printed at the center conductor of the CPW. All the designs reported in [12-16] required extra structures for mode convergence, including λ/2 phase shifter [14] and λ/4 matching structures [12-13, 15], which occupy considerable space in the feed network.

In this paper, a compact switchable CPW-to-slotline transition without any extra structures is proposed and can be treated as an improvement from the design reported in [17]. The proposed CPW-to-slotline transition provides three feed modes: CPW feed, LS feed and RS feed, and is utilized to feed a wideband Vivaldi notched monopole, which is studied in [12]. In this case, the reconfigurable pattern is realized by switching the feed modes in the working frequency range from 4–6 GHz. Compared to the antenna discussed in [12], smaller dimensions of feed structure are realized. Only 2 p-i-n diodes are used in the proposed design, which is less than the 4 p-i-n diodes used in [12]. As a result, the bias circuit is simpler and the parasitic

This work is supported by the National Basic Research Program of China under Contract 2010CB327402, in part by the National High Technology Research and Development Program of China (863 Program) under Contract 2009AA011503, the National Science and Technology Major Project of the Ministry of Science and Technology of China 2010ZX03007-001-01 and Qualcomm Inc..

Y. Li, Z. Zhang, J. Zheng, and Z. Feng are with State Key Laboratory on Microwave and Digital Communications, Tsinghua National Laboratory for Information Science and Technology, Department of Electronic Engineering, Tsinghua University, Beijing, 100084, China (e-mail: zjzh@tsinghua.edu.cn)

M. F. Iskander is with the Hawaii Center for Advanced Communications (HCAC), University of Hawaii at Manoa, Honolulu, HI 96822 USA (e-mail: iskander@spectra.eng.hawaii.edu).

parameters as well as the insertion loss introduced by p-i-n diodes are all reduced in the proposed design. A prototype of the proposed antenna is simulated and fabricated. The reflection coefficients, radiation patterns and gains of three feed modes are measured. In order to confirm the benefits of the pattern diversity in multiple antennas systems, the channel capacity of a 2x2 antenna array is measured in a typical indoor environment. Compared to the standard omni-directional dipoles, the improvement of spectral efficiency is achieved by using the proposed antenna in both LOS and NLOS communication scenarios.

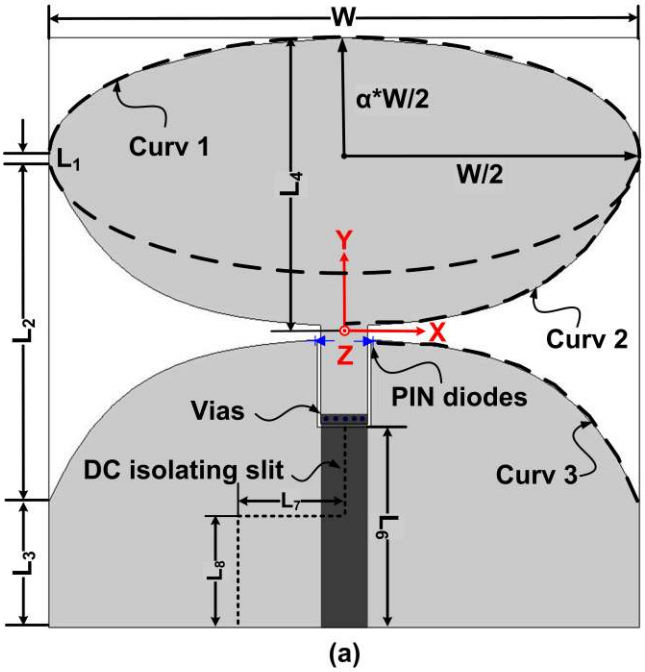

Fig. 1. Geometry and configuration of the proposed antenna. (a) Front view; (b) Detailed view of feed structure.

TABLE I
WORKING CONFIGURATION OF PIN 1 AND PIN 2

PIN 1	PIN 2	Feed
OFF	OFF	CPW
OFF	ON	LS
ON	OFF	RS

II. ANTENNA DESIGN PRINCIPLE

A. Antenna configuration

The configuration of the proposed antenna is shown in Fig. 1 (a). As it may be seen, it is composed of an elliptical topped monopole, two Vivaldi notched slots and a typical CPW feed with two p-i-n diodes. The antenna is printed on the both sides of a 50 x 50 mm^2 Teflon substrate, whose relative permittivity is 2.65 and thickness is 1.5 mm. The CPW is connected to the microstrip at the back side through vias. A 0.2 mm wide slit is etched on the ground at the front side for DC isolation. Three curves are used to define the shape of antenna, fitted to the coordinates in Fig. 1 (a):

Curve 1:

$$(\frac{x}{W/2})^2+[\frac{y-(L_4-\alpha*W/2)}{\alpha*W/2}]^2=1 \quad (1)$$

where $L_4-\alpha*W/2\le y\le L_4$, and $\alpha=0.4$.

Curve 2 [18]:

$$y=C_1e^{c\cdot x}+C_2 \quad (2)$$

where $C_1=14, C_2=0.26, c=0.16$. Values of these parameters are chosen after optimization. Curve 3 and curve 2 are symmetrical along X axis

B. Compact CPW-slot transition

In order to achieve reconfigurable patterns, a switchable CPW-to-slotline transition with 2 p-i-n diodes is used as shown in Fig. 1 (b). This feed structure is able to switch from CPW feed to slotline feed by controlling the bias voltage of p-i-n diodes. The working configurations of the two p-i-n diodes (PIN 1 and PIN 2) are listed in TABLE I. When both p-i-n diodes are in the state of 'OFF', the elliptical topped monopole is fed through a typical CPW and a nearly omni-directional radiation pattern is achieved in XZ plane. When PIN 1 is 'OFF' and PIN 2 is 'ON', the right slotline is shorted. The left Vivaldi notched slot is fed through the left slotline of the CPW, and a unidirectional radiation pattern is formed along the –X axis. In the same way, when PIN 1 is 'ON' and PIN 2 is 'OFF', a unidirectional beam along the +X axis is achieved in the right Vivaldi notched slot through the Right Slot (RS) feed. As a result, the reconfigurable patterns are realized by switching the modes in the CPW with two p-i-n diodes.

The proposed CPW-to-slotline transitions are designed in a compact size to reduce the overall dimensions of the antenna. An equivalent transmission line model is used to explain the

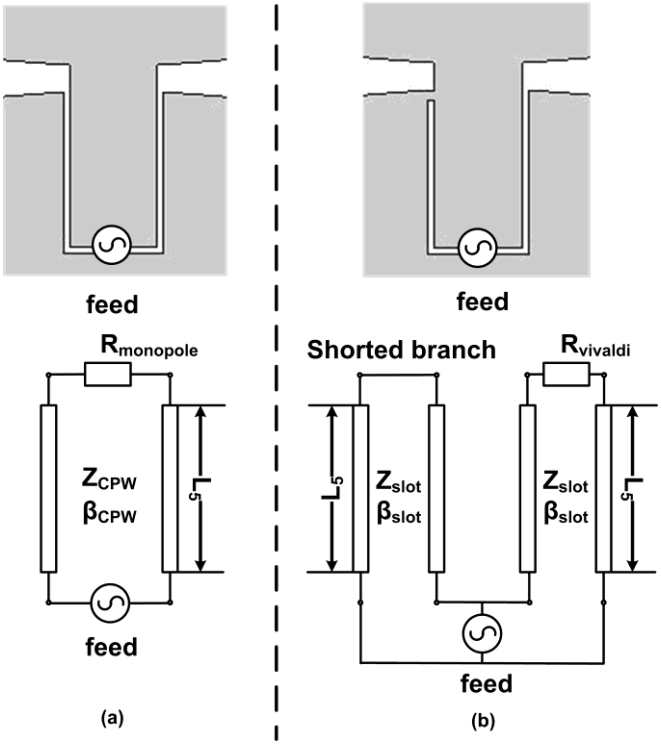

Fig. 2. Feed diagram and equivalent transmission line model. (a) CPW feed; (b) RS feed.

TABLE II
DETAILED DIMENSIONS OF THE PROPOSED ANTENNA

Parameter	L_1	L_2	L_3	L_4	L_5	L_6
Value (mm)	1.74	28.52	10.74	25	8	16.8
Parameter	L_7	L_8	L_p	W	W_1	S_1
Value (mm)	10	10	2	50	4	0.3

feed transition and the p-i-n diode is expressed as perfect conductor for 'ON' state and open circuit for the 'OFF' state. Fig. 2 (a) shows the typical CPW feed, the length of L_5 is tuned to match the radiation resistance $R_{monopole}$ of monopole from 50Ω at the feed port. When a slotline on either side of the CPW is shorted by p-i-n diode, the feed diagram and equivalent transmission line model of RS feed are depicted in Fig. 2 (b). The right slotline is used to feed the Vivaldi notched slot, and the shorted left slotline works as a matching branch. Some related approaches are given in [13] but the proposed method is significantly different as we don't use any extra matching structures. The shorted branch which is less than a quarter of wavelength serves as a shunt inductance and its value is determined by its length. As an improvement from the matching discuss in [16], the locations of p-i-n diodes are not fixed, as shown in Fig. 3. Therefore, the value of shunt inductance $jZ_{slot}\tan[\beta slot(L_1\text{-}Lp)]$ can be tuned for a better matching. As a result and by optimizing the length of L_5 and L_p, the radiation resistance $R_{Vivaldi}$ will be well matched to 50Ω. What is more important is the fact that we only use two p-i-n diodes to control

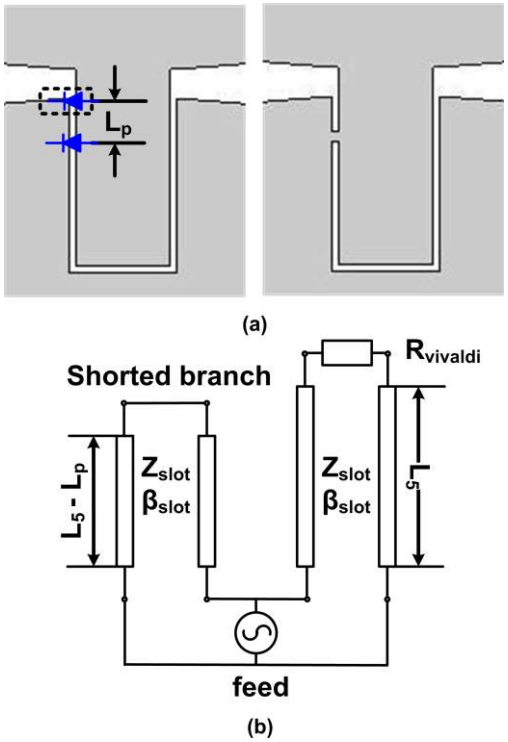

Fig. 3. Matching strategy of RS feed. (a) Feed diagram; (b) Equivalent transmission line model.

the transition instead of 4 as described in [12]. Therefore, smaller dimension of antenna is realized by using compact feed and simple bias circuit. To help evaluate the developed antenna one may make parametric study such as those described in [19], and conduct experimental validation as described in Section III and IV of this paper. The values of parameters are optimized by using the software Ansoft High Frequency Structure Simulator (HFSS). The optimized values are listed in TABLE II.

III. ANTENNA FABRICATION AND EXPERIMENTAL RESULTS

In order to validate the design of the compact switchable CPW-to-slotline transition, a prototype of the proposed antenna with bias circuit is built and tested, as shown in Fig. 4. The selected p-i-n diode is Agilent HPND-4038 beam lead PIN diode, with acceptable performance in a wide 1-10 GHz bandwidth. When the p-i-n diode is forward-biased, it can be treated as a series resistance. The insertion loss introduced by p-i-n diodes is approximately 0.3 dB at its typical bias current of 5-10 mA. That is to say, the efficiency decreases 0.3 dB by using p-i-n diodes. When the p-i-n diode is reverse-biased, on the other hand, it is replaced by a series capacitance of approximately 0.06 pF, which will shift the working frequency

of the antenna but with less insertion loss. As a result, the insertion loss mainly comes from the p-i-n diodes at 'ON' state for CPW mode. Clearly, a reduced number of p-i-n diodes will reduce the insertion loss and improve the performance of the systems. The detailed bias configuration of p-i-n diodes is

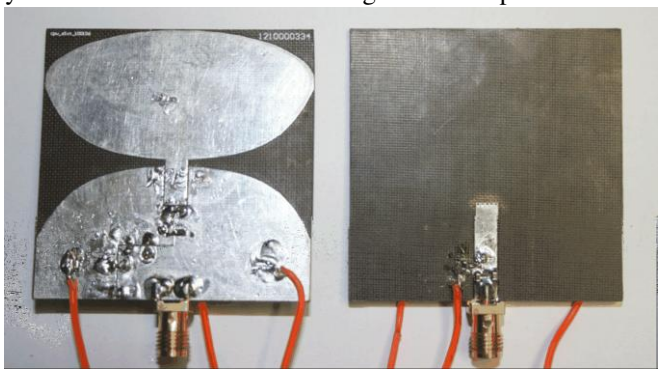

Fig. 4. Fabrication of the proposed antenna.

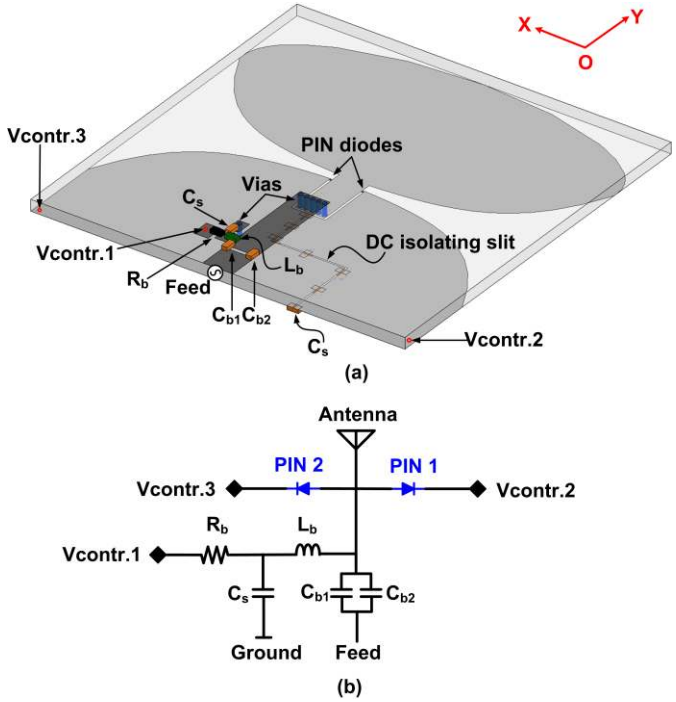

Fig. 5. Bias configuration of p-i-n diodes. (a) 3-D view, (b) back view.

shown in Fig. 5. Specifically, Fig. 5 (a) shows the 3-D view of bias circuit. The slit is etched on the front side to isolate the bias voltage of two p-i-n diodes. Several capacitances (C_s) are soldered over the slit for RF short. The radius of the vias, connecting the front and back sides, is 0.3 mm. In Fig. 5 (b), the complete circuit diagram is illustrated. Vcontr.1, Vcontr.2 and Vcontr.3 use 3.3 V bias voltages to control the states of the two p-i-n diodes. Another capacitance is used between Vcontr.1 and the ground, in order to short the RF signal leaked from the choking inductance (L_b). Therefore, the cable of Vcontr.1 has little effect to the antenna performance. The bias circuit of p-i-n diodes is on the back side. The bias resistance (R_b) is 430 Ω; with the bias current is 7.7 mA. The RF choking inductance (L_b) is 10 nH. The RF signal shorting capacitances (C_s) are all 470 pF, and the DC block capacitances (C_{b1} and C_{b2}) are 20 pF each. All the measurements were taken using an Agilent E5071B network analyzer. The simulated and measured reflection coefficients of CPW feed, LS and RS feeds are shown in Fig. 6

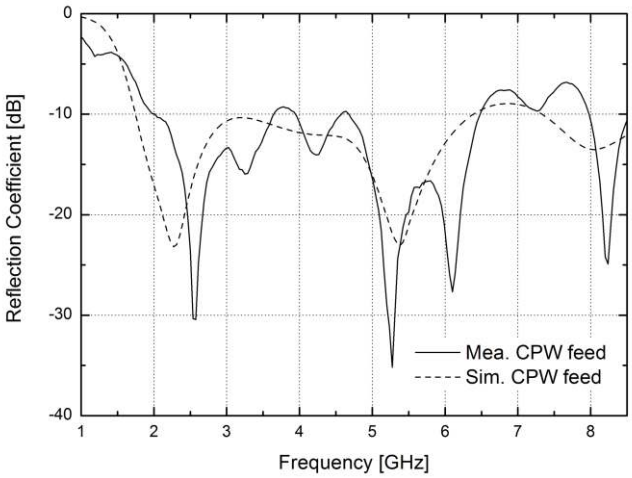

Fig. 6. Simulated and measured reflection coefficients of CPW feed

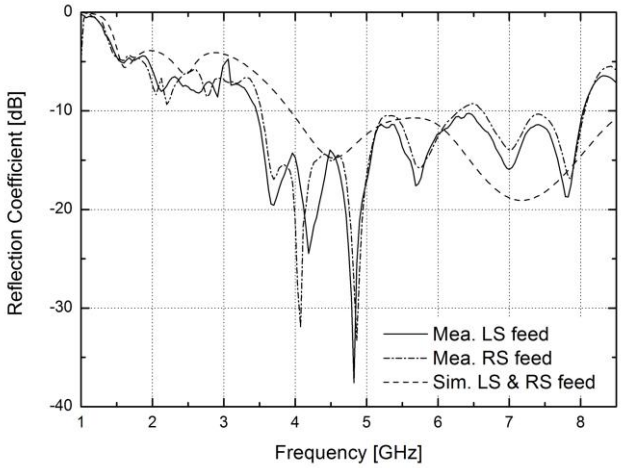

Fig. 7. Simulated and measured reflection coefficients of slotline feed.

and Fig. 7. The difference between simulated and measured results is introduced by the parasitic parameter and loss of the p-i-n diodes bias circuit. The measured -10dB bandwidths are 2.02-6.49 GHz, 3.47-8.03 GHz and 3.53-8.05 GHz for CPW feed, LS feed and RS feed, respectively. The overlap band from 3.53 GHz to 6.49 GHz is treated as the operation frequency for reconfigurable patterns.

The measured radiation pattern in XZ and XY planes for CPW feed, LS feed and RS feed at 4, 5, 6 GHz are listed in TABLE III and IV. The results are normalized by the maximum value of each mode at each frequency point. For the CPW feed, a nearly omni-directional radiation pattern is achieved in XZ plane and a doughnut shape in XY plane. For the LS or RS feed,

a unidirectional beam is achieved along –X or +X axis, with acceptable front-to-back ratio better than 9.5dB. The different patterns of radiation are able to be switched dynamically according to the environment, proving the pattern diversity.

The measured gains of CPW, LS and RS feed are illustrated in Fig. 8. The maximum value in the XY and XZ plane is selected as the gain of each mode. For the CPW feed, an average gain in the desired frequency range is 2.92 dBi. For the LS and RS feed, the average gains in the 4-6 GHz band are 4.29 dBi and 4.32 dBi. The improved gain is mainly contributed to the directivity of the slotline feed mode, and the diversity gain is achieved by switching the patterns.

TABLE III
MEASURED NORMALISED RADIATION PATTERN IN XZ PLANE

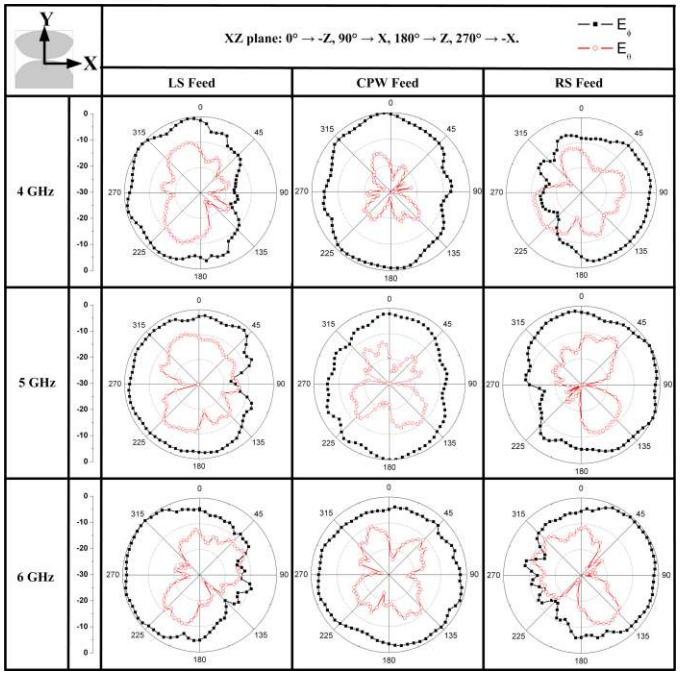

TABLE IV
MEASURED NORMALISED RADIATION PATTERN IN XY PLANE

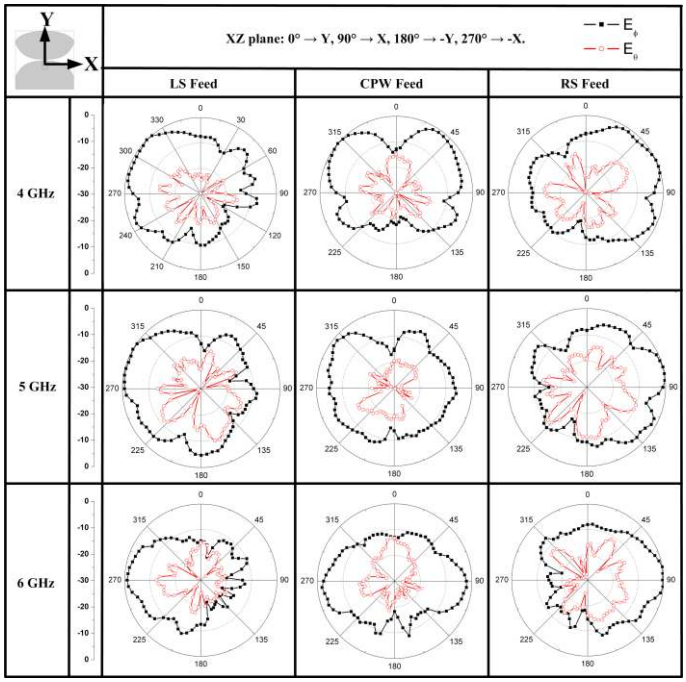

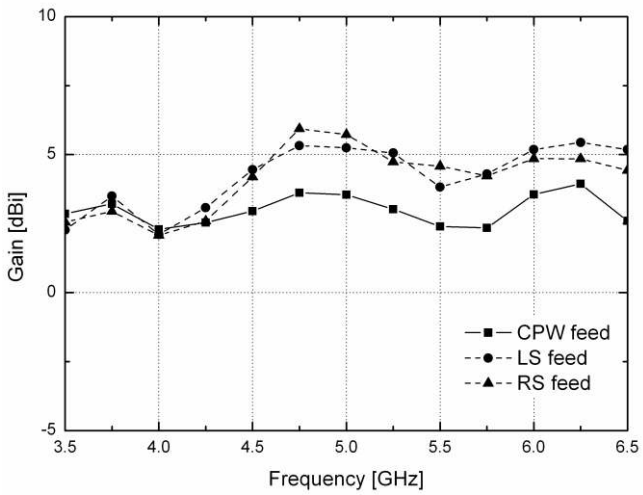

Fig. 8. Measured gains of antenna through different feed

IV. CHANNEL CAPACITY MEASUREMENT

A. *Measurement setup*

In this section, we describe the experimental procedure we used to test and validated advantages of using the developed antenna system in improving channel capacity in an indoor propagation environment. To this end, the channel capacity of a 2x2 multiple antenna system is measured. The antenna array consists of two proposed reconfigurable antennas at receive end and the reference two-dipole array at transmit end. The elements of the reference two-dipole array are arranged perpendicular to XZ plane along X axis. Each port of the two wire dipoles has a bandwidth of 3.9-5.9 GHz with reflection coefficient better than –6 dB, and mutual coupling between the two ports is lower than –25 dB over the frequency band which is achieved by tuning the distance between two elements. Also, the isolation between two proposed antennas is lower than –25 dB.

The measurement system consists of an Agilent E5071B network analyzer, which has 4 ports for simultaneous measurement, transmit antennas, receive antennas, RF switches, a computer and RF cables. The transmit antennas and the receive antennas are connected to the ports of the network analyzer, respectively. The computer controls the measurement procedure and records the measured channel responses. The measurement was carried out in a typical indoor environment in the Weiqing building of Tsinghua University, shown in Fig. 9. The framework of the room is reinforced concrete, the walls are mainly built by brick and plaster, and the ceiling is made with plaster plates with aluminium alloy framework. The heights of

desk partition and wood cabinet are 1.4 m and 2.1 m. The transmit antenna array is fixed in the middle of room (TX). The receive antenna array is arranged in several typical locales which are noted as RX1-4 in Fig. 9. Here, the scenarios when the receive antenna array is arranged in RX2 and RX3 are LOS, while that is NLOS when the receive antenna array is arranged in RX1 and RX4. In the measured, the antennas used are fixed at the height of 0.8 m.

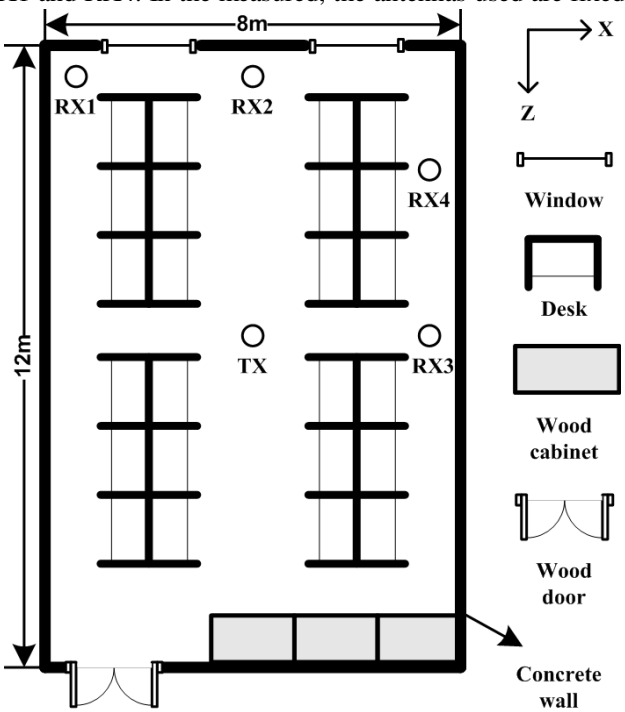

Fig. 9. Indoor environment for channel capacity measurement.

TABLE V
AVERAGE AND 95% OUTAGE CHANNEL CAPACITY (BIT/S/HZ)

Channel Capacity	Measurement Scenario	1x1 Dipole	2x2 Dipole	2x2 Pattern Reconfig.
Average	LOS	5	9.46	11.74
	NLOS	5	9.93	13.06
95% Outage	LOS	2.29	4.21	6.72
	NLOS	1.68	5.41	9.16

The measured data was taken in the frequency range of 4-6 GHz, with a step of 10 MHz. A total number of 201 data points/results are obtained in a typical sampling. Three configurations (CPW, LS and RS) of each element of the receiver array were switched together manually and the strongest receive signal was selected for statistics. Considering the small-scale fading effect, 5x5 grid locations for each RX position were arranged. As a result, a total number of 2x201x25 = 10050 results were measured for statistics in LOS and NLOS scenario respectively. In a real scenario, the three modes of the proposed antenna can be electrically controlled by a chip depending on the strength of receiving signal.

In order to validate the effect of the proposed antennas for the systems, the channel responses of the system with another two reference dipoles used as the receive antennas instead of the pattern reconfigurable antennas in the same measurement arrangements are measured and recorded for comparison.

In the measurement, a 2x2 channel matrix H is obtained. The channel capacity is calculated by formula (3).

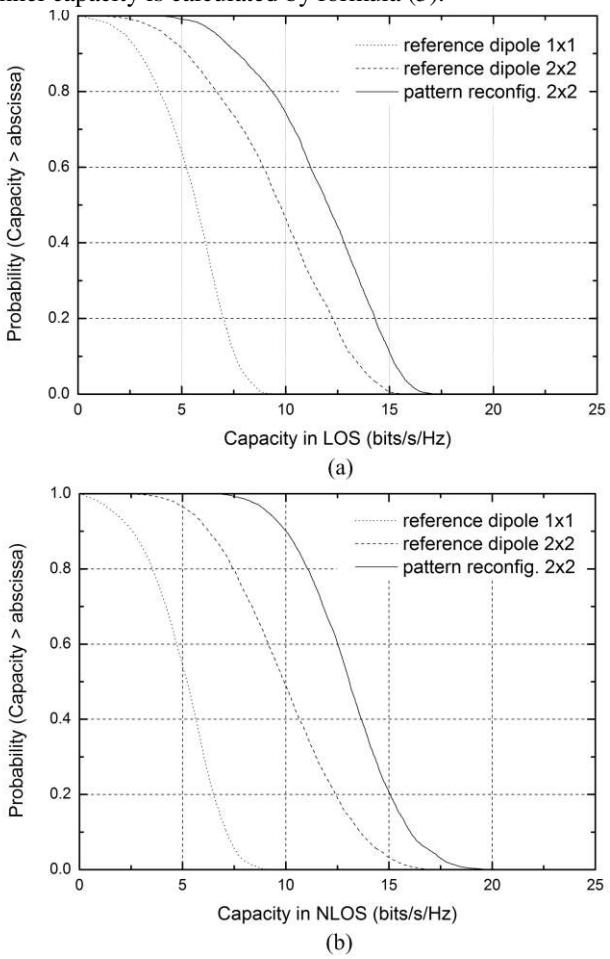

Fig. 10. CCDFs of channel capacity. (a) LOS scenario; (b) NLOS scenario.

$$C = \log_2 \det[I_{N_r} + \frac{SNR}{N_t} H_n H_n^H] \quad (3)$$

where N_r and N_t are the numbers of receiver and transmitter antennas. H_n is the normalized H by the received power in the reference dipole system, and $()^H$ means the Hermitian transpose. I_{Nr} is an N_r x N_r identity matrix, and SNR is the signal-to-noise ratio. We selected the SNR when the average channel capacity is 5 bit/s/Hz in a 1x1 reference dipole system in LOS or NLOS scenario.

B. Channel capacity results

Fig.10 shows the measured Complementary Cumulative Distribution Function (CCDF) of channel capacity in LOS and NLOS scenarios. The results consist of the channel capacity information of 2x2 multiple antenna system using the proposed

pattern reconfigurable antennas, compared with 1x1 and 2x2 systems using reference dipoles. As listed in TABLE V, 2.28 bit/s/Hz and 4.13 bit/s/Hz of the average capacity improvement are achieved in LOS and NLOS scenarios, and 2.51 bit/s/Hz and 3.75 bit/s/Hz improvement for 95% outage capacities. In the NLOS scenario, the received signal is mainly contributed from reflection and diffraction of the concrete walls and the desk partitions, arriving at the direction of endfire. The diversity gain in the endfire increases the channel capacity. However, the path loss of NLOS is higher than that of LOS, and the transmitting power should be enhanced to ensure the performance of the system. Considering the insertion loss introduced from non-ideal p-i-n diodes, better performance of the proposed antenna can be achieved by using high quality switches, such as micro-electro-mechanical systems (MEMS) type switches with less insertion loss and smaller parasitic parameters.

V. Conclusion

A compact switchable CPW-to-slotline transition feed without extra matching structures is proposed in this paper to design a wideband reconfigurable system. CPW, LS and RS feed modes are provided to feed an elliptical topped monopole with a pair of Vivaldi notched slots for reconfigurable patterns. A nearly omni-directional pattern is achieved by feeding the monopole through CPW feed, and two endfire patterns are achieved by feeding the Vivaldi notched slots through slotline feed. An equivalent transmission line model is used to analyze the feed structure. The feed modes are controlled by only two p-i-n diodes. A prototype of the proposed antenna is fabricated and tested to prove the adequacy of the feed design. Specifically, a wide bandwidth of 3.53-6.49 GHz is achieved for reconfigurable pattern with the reflection coefficient lower than -10 dB. The radiation patterns of each feed mode are measured to demonstrate the successful achievement of the pattern diversity. The average gain improvement in the direction of endfire is better than 1.37 dB in the operation band. To prove the benefit of diversity gain, the channel capacity of a 2x2 multiple antenna system using the proposed antennas is measured in an indoor propagation environment. Compared with reference wire dipoles in the same measurement, the average and 95% outage capacities are both improved by using the proposed antennas, especially in a NLOS scenario.

Reference

[1] Daniele Piazza, Prathaban Mookiah, Michele D'Amico and Kapil R. Dandekar, "Experimental Analysis of Pattern and Polarization Reconfigurable Circular Patch Antennas for MIMO Systems," IEEE Trans. Veh. Technol., vol. 59, no. 5, pp. 2352–2363, Jun. 2010.

[2] M. Sanchez-Fernandez, E. Rajo-Iglesias, O. Quevedo-Teruel, and M. Luz Pablo-González., "Spectral Efficiency in Mimo Systems Using Space and Pattern Diversities under Compactness Constraints," Vehicular Technology, IEEE Transactions on, vol. 57, pp. 1637-1645, 2008.

[3] Joshua D. Boerman and Jennifer T. Bernhard, "Performance Study of Pattern Reconfigurable Antennas in MIMO Communication Systems," IEEE Trans. Antennas Propag., vol. 56, no. 1, pp. 231–236, Jun. 2008.

[4] Greg H. Huff, and Jennifer T. Bernhard, "Integration of packaged RF MEMS switches with radiation pattern reconfigurable square spiral microstrip antennas," IEEE Trans. Antennas Propag., vol. 54, no. 2, pp. 464–469, Feb. 2006.

[5] Prafulla Deo, Amit Mehta, Dariush Mirshekar-Syahkal, and Hisamatsu Nakano, "An HIS-Based Spiral Antenna for Pattern Reconfigurable Applications," IEEE Antennas and Wireless Propag. Letters, vol. 8, pp. 196–199, 2009.

[6] Shing-Hau Chen, Jeen-Sheen Row, and Kin-Lu Wong "Reconfigurable Square-Ring Patch Antenna With Pattern Diversity," IEEE Trans. Antennas Propag., vol. 55, no. 2, pp. 492–475, Feb. 2007.

[7] Xue-Song Yang, Bing-Zhong Wang, Weixia Wu and Shaoqiu Xiao, "Yagi Patch Antenna With Dual-Band and Pattern Reconfigurable Characteristics," IEEE Antennas and Wireless Propag. Letters, vol. 6, pp. 168–171, 2007.

[8] S. Zhang, G. H. Huff, J. Feng, and J. T. Bernhard, "A Pattern Reconfigurable Microstrip Parasitic Array," IEEE Trans. Antennas Propag., vol. 52, no. 10, pp. 2773–2776, Oct. 2004.

[9] Julien Sarrazin, Yann Mahé, Stéphane Avrillon, and Serge Toutain, "Pattern Reconfigurable Cubic Antenna," IEEE Trans. Antennas Propag., vol. 57, no. 2, pp. 310–317, Feb. 2009.

[10] Angus C. K. Mak, Corbett R. Rowell, and Ross D. Murch, "Low Cost Reconfigurable Landstorfer Planar Antenna Array," IEEE Trans. Antennas Propag., vol. 57, no. 10, pp. 3051–3061, Oct. 2009.

[11] I-Young Tarn and Shyh-Jong Chung, "A Novel Pattern Diversity Reflector Antenna Using Reconfigurable Frequency Selective Reflectors," IEEE Trans. Antennas Propag., vol. 57, no. 10, pp. 3035–3042, Oct. 2009.

[12] Sung-Jung Wu and Tzyh-Ghuang Ma, "A Wideband Slotted Bow-Tie Antenna With Reconfigurable CPW-to-Slotline Transition for Pattern Diversity," IEEE Trans. Antennas Propag., vol. 56, no. 2, pp. 327–334, Feb. 2008.

[13] H. Kim, David Chung, D. E. Anagnostou, and John Papapolymerou, "Hardwired Design of Ultra-Wideband Reconfigurable MEMS Antenna", IEEE, Personal, Indoor and Mobile Communications, PIMRC2007, 18th Annual Intl' Symp on, September 3-7, 2007.

[14] Kuang-Ping Ma, Yongxi Qian, and Tatsuo Itoh, "Analysis and applications of a new CPW-slotline transition," IEEE Trans. Microwave Theory Tech., vol. 47, pp. 426–432, Apr. 1999.

[15] Yo-Shen Lin and Chun Hsiung Chen, "Design and modeling of twin-spiral coplanar-waveguide-to-slotline transitions," IEEE Trans. Microwave Theory Tech., vol. 48, pp. 463–466, Mar. 2000.

[16] Khelifa Hettak, Nihad Dib, A. Sheta, Amjad A. Omar, Gilles-Y. Delisle, Malcolm Stubbs, and Serge Toutain, " New miniature broadband CPW-to-slotline transitions," IEEE Trans. Microwave Theory Tech., vol. 48, pp. 138–146, Jan. 2000.

[17] Yue Li, Zhijun Zhang, Wenhua Chen and Zhenghe Feng, "Polarization Reconfigurable Slot Antenna with a Novel Compact CPW-to-Slotline Transition for WLAN Application," IEEE Antennas and Wireless Propag. Letters, IEEE Antennas and Wireless Propag. Letters, vol. 9, pp. 252–255, 2010.

[18] J. Shin and D. H. Schaubert, "A parameter study of stripline-fed Vivaldi notch-antenna arrays," IEEE Trans. Antennas Propag., vol. 47, pp. 879–886, May 1999

[19] Yue Li, Zhijun Zhang, Zhenghe Feng, Magdy Iskander and Ruihong Li, 'A Wideband Pattern Reconfigurable Antenna With Compact Switchable Feed

Structure', International Conference on Microwave and Millimeter Wave Technology, Chengdu, China, pp. 1–4, May, 2010.